THE EUROPEAN SOCIETY OF MEDICINE
Medical Research Archives, Volume 14 Issue 3

RESEARCH ARTICLE

Investigating the Role of Temperature and Surfactant Saturation in Triton X-100 Mediated Proteoliposome Production

Sarah McColman[1,2] and David T. Cramb[1,2,*]

[1]Department of Chemistry and Biology, Faculty of Science, Toronto Metropolitan University, 350 Victoria Street, Toronto, ON M5B 2K3, Canada
[2]Institute for Biomedical Engineering, Science, and Technology (iBEST) – Li Ka-Shing Knowledge Institute at St. Michael's Hospital - Unity Health Toronto, 209 Victoria Street, Toronto, ON M5B1T8, Canada

OPEN ACCESS

PUBLISHED
31 March 2026

CITATION
McColman, S. and Cramb, D.T., 2026. Investigating the Role of Temperature and Surfactant Saturation in Triton X-100 Mediated Proteoliposome Production. Medical Research Archives, [online] 14(3).

ISSN
2375-1924

ABSTRACT

Reconstituting membrane proteins into liposomes to form proteoliposomes is an essential tool for studying structural and functional properties of these biomolecules. Detergent-mediated reconstitution is a well-established method of inserting these membrane-anchored proteins into liposome membranes, but limited data has been published investigating the role of temperature in this process. In this study, the temperature at which multicomponent liposomes are saturated with Triton X-100, a commonly used nonionic detergent, was manipulated during the reconstitution protocol of a model protein, SARS-CoV-2 Spike glycoprotein. Several parameters were monitored across different saturation temperatures: the concentration of detergent required to saturate these liposomes, the amount of polystyrene adsorbent "BioBeads" required to remove the detergent from the liposomes, and the physical properties of resulting particles, including the average number of proteins inserted in each proteoliposome. The temperature-dependence of Triton X-100 saturation of the liposomes investigated here was found to be minimal beneath 60 °C, and a saturation ratio range of 4.6-9.2 moles Triton X-100 per mole of lipid was required to saturate these multicomponent particles. Removal of Triton X-100 by BioBeads was similarly unaffected by the saturation temperature. Importantly, the cloud point behaviour of Triton X-100 was implicated in the aggregation of liposomes and proteoliposomes. Localization of proteins within particle-aggregate dispersions suggests that while saturation temperature does not seem to influence the density of proteins reconstituted in each proteoliposome, at elevated temperatures the aggregation effect reduces the total yield of proteoliposomes. The approach presented here provides a framework for improving and assessing detergent-mediated protein reconstitution processes and suggests key factors to consider for experimental design of proteoliposome preparation.

Keywords: Liposomes; viruses; temperature; formulation; size; stability

1. Introduction

Reconstituting proteins into synthetic membrane models has been an important strategy to study membrane protein activity and structure since the 1960s. While membrane proteins can be stabilized in various membrane-mimicking forms such as in detergent micelles, lipid-detergent bicelles, and copolymer nanodisc structures[1–3], liposomes remain essential for membrane protein biochemical studies and analysis. For example, protein-containing liposomes ("proteoliposomes") are useful for structural determination of membrane proteins[4,5], transmembrane transport assays of ions and molecules[6–11], and for modeling cell membranes or enveloped viruses[12,13]. Recent increased biopharmaceutical interest in the therapeutic potential of extracellular vesicles (EVs) has also led to advances in proteoliposome development, particularly for their application as synthetic EVs or EV-mimicking drug carriers[14–18]. Reconstitution of membrane proteins into liposomes to form proteoliposomes has been reported in literature using various methods. One so-called "detergent-free" method utilizing copolymer nanodisc-solubilized membrane proteins was recently reported to successfully reconstitute proteins into lipid vesicles[19]. By far the most common method to form proteoliposomes, however, is the use of surfactants to facilitate the insertion of proteins into liposome membranes in what are termed detergent-mediated reconstitution protocols[20–22].

A canonical mechanism for detergent – liposome interactions is described in three stages: as detergent is added to a liposome solution, the surfactant monomers insert into the membrane of unsaturated liposomes (stage I) until the liposomes are saturated with the detergent (stage II)[23]. After this, if more detergent is added to the system, besides the formation of micelles comprised purely of detergent monomers, the liposome membranes which are saturated and unable to accommodate more detergent will begin to solubilize into mixed lipid-detergent micelles (stage III) until no intact liposomes are present (see Figure 1)[23]. The least common detergent-mediated reconstitution method involves only the detergent present in the solubilized membrane protein solution; allowing the membrane proteins solubilized in detergents to mix with intact liposomes (in stage I), after which the removal of the protein-solubilizing detergent prompts the reconstitution of the protein into the vesicle[24,25]. A more typical method, introducing the membrane proteins to mixed micelles (liposomes in stage III), has been demonstrated for reconstituting transporter proteins such as ammonia transporters[26], glutamine transporters[6], carnitine transporters[7], and Ca2+ ATP-ases[27,28] into proteoliposomes. Other proteins important to cellular processes such as cellulose synthase[29,30] and photosystem proteins[30], as well as proteins implicated in pathogens such as M. tuberculosis[31] have been reconstituted into liposomes in this way as well. A drawback of fully solubilizing liposomes before reconstituting proteins into the membranes is that the orientation of the reconstituted proteins becomes randomized which can affect activity of the protein if that is to be assayed[32]. In addition, the use of fully solubilized liposomes to reconstitute proteins has been shown to lead to problematic aggregation of reconstituted species which can also impact the structure and function of proteins of interest[33].

To circumvent this issue, researchers can use liposomes that have been only saturated, but not yet solubilized, with detergent. Examples of this in literature are the reconstitutions of transport proteins[27,33], ATPases and fusion proteins[34,35], and recently glycoproteins from coronaviruses such as SARS-CoV-2[36,37]. Literature on protein reconstitution using Triton X-100 to saturate liposomes generally does not make note of the temperature at which liposomes are saturated by detergents. Previously, reconstitution of SARS-CoV-2 spike glycoproteins into biomembrane-mimicking liposomes was conducted by the Cramb group[36]. These reconstitutions were performed by saturating the liposomes at room temperature, because of anecdotal evidence of aggregate formation when saturation was completed at elevated temperatures (unpublished data), and these observations led to

this current work. The goal of the present study was to understand any relationship between the temperature used during Triton X-100 saturation of liposomes and the resulting particle properties, for a liposome comprised of multiple lipid components with different physicochemical properties and regions of different fluidity at room temperature. More specifically, in this work we were interested in investigating how the temperature of saturation of such particles by Triton X-100 might impact the molar ratio of detergent to lipid required for saturation (Rsat), the ability of similar Triton X-100 concentrations to be removed from a solution using Bio-Bead adsorbents, and the degree to which proteins are incorporated into the liposomes after the completion of the reconstitution protocol.

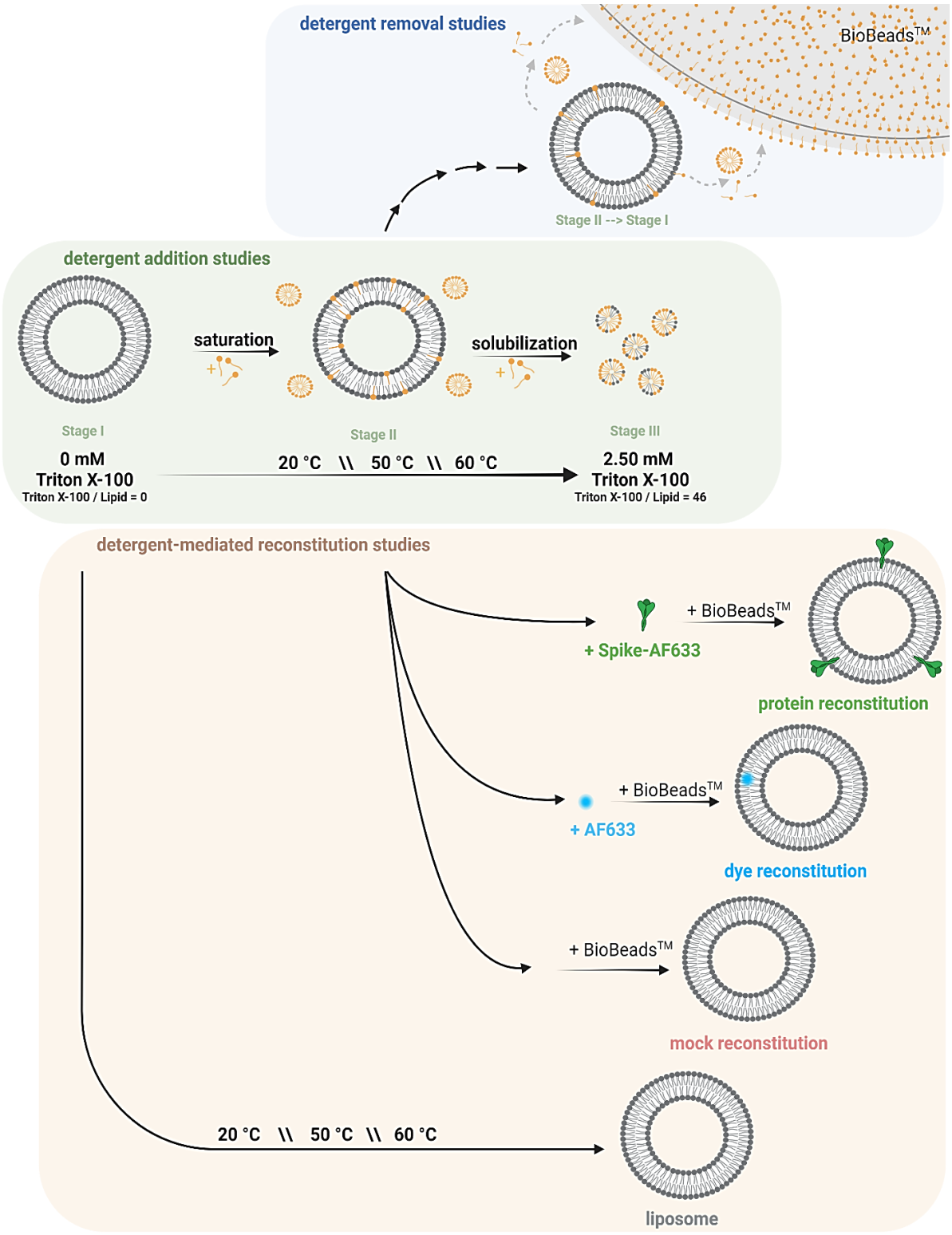

Figure 1. Schematic of experimental design broken into three stages: detergent addition, detergent removal, and reconstitution.

2. Materials

1,2-Dioleoyl-sn-glycero-3-phosphocholine (DOPC), 2-dipalmitoyl-sn-glycero-3-phosphoethanolamine (DPPE), and cholesterol were purchased from Millipore Sigma (Oakville, Ontario, Canada). 1,2-dipalmitoyl-sn-glycero-3-phospho-(1′-myo-inositol) (DPPI) was purchased from Cayman Chemical. Stock solutions were prepared in chloroform (or 1:1 v/v methanol to chloroform for DPPE) and stored at -20 °C. Full-sequence SARS-CoV-2 spike glycoprotein trimers solubilized in LMNG detergent micelles were purchased from Cube Biotech (Monheim am Rhein, Germany) and fluorescently labeled with AlexaFluor-633 labeling kits from Thermo Fisher Scientific, Inc. (Mississauga, ON, Canada). Earl's Balanced Salts Solution (EBSS) and Triton X-100 were purchased from Millipore Sigma. Bio-Beads SM-2 resin (hereafter, Bio-Beads) was purchased from Bio-Rad (Mississauga, ON, Canada). Sodium azide was purchased from Millipore Sigma and lauryl maltose neopentyl glycol (LMNG) detergent was purchased from Anatrace (Maumee, OH, USA).

3. Methods

3.1. LIPOSOME PREPARATION:

Unilamellar liposomes were prepared using thin-film hydration as reported elsewhere[36]. Briefly, lipid components combined in chloroform were desolvated under nitrogen gas and rehydrated in EBSS at 60 °C. EBSS was selected as the buffer based on its compatibility with *in vitro* cell treatments performed in a previous study using the same liposome formulation[36]. The liposomes were extruded through 100 nm – pore polycarbonate filters at 60 °C and extruded liposomes (10x) were diluted tenfold in EBSS at 20 °C to obtain the final sample (1x).

Table 1. Formulation of liposomes used in this study as prepared (10x) before dilution to 1x working solution. Full set of membrane component compositions throughout different study sections can be found in Supplementary Table S1. For rationale behind this formulation see McColman et al., 2023 in which we describe the selection of these lipid compositions in the formulation as an attempt to approximate the composition of lipids within the SARS CoV-2 viral membrane.

Membrane Component *Abbr (a:b PX)**	Lipid Melting temperature	Headgroup			% of membrane content		Concentration (10x)	
	T_m (°C)	pKa (HPO_4)[31]	pKa (R)[31]	Charge at pH 7[31]	Mol %	Mass %	µM	µg/mL
DOPC (18:1 PC)	-16.5[32]	1.0	n/a	Neutral	77.5	80.9	676.0	496.0
DPPE (16:0 PE)	61-64[33]	1.7	11.25	Neutral	8.7	8.7	76.0	53.0
DPPI (16:0 PI)	40.9[34]	2.5	n/a	-1	4.6	5.4	40.0	33.0
Cholesterol					9.2	5.1	80.0	31.0
Total							**872.0**	**613.0**

* Abbr = abbreviated lipid name, a = acyl chain length, b = degree of unsaturation in each tail chain, PX = glycerophosphatidyl headgroup where X is C (choline), E (ethanolamine), or I (inositol).

3.2. PROTEIN FLUORECENT LABELING

Spike glycoproteins in LMNG micelles were pH-adjusted to approximately pH 8 using sodium bicarbonate. This protein was added to a vial of reactive Alexa Fluor 633 dye and this succinimide ester-based conjugation mixture was stirred at 20 °C for 90 min. The reaction mixture was then added to a 30 kDa molecular weight cut-off dialysis cassette and dialyzed for 48 h against excess 1x PBS supplemented with 2 mM sodium azide and 5 µM lauryl maltose neopentyl glycol (LMNG) detergent. After dialysis, the sample (Spike-LMNG-AF633) was collected and the concentration and degree of labeling of the protein was determined by measuring absorbance at 280 nm and 632 nm using a NanoDrop™ spectrophotometer. Control experiments were reported by us elsewhere illustrating the lack of notable interference of this label with spike glycoprotein structure or function[36].

3.3. BIO-BEAD PREPARATION AND TREATMENTS

Bio-Beads were prepared according to the manufacturer's protocol. Briefly, Bio-Beads were washed twice for 20 min in spectrophotometric grade methanol. Following these two washes, the beads were washed twice for 20 min with Millipore water. Standard quantities of Bio-Beads to achieve prescribed wet bead mass were approximated by weighing 10-15 beads on an analytical balance and visualizing that quantity on a scoopula. For each Bio-Bead treatment, two rounds of 3 mg of beads were added by scoopula and shaken on a rotary shaker for two hours at room temperature. After these four hours, a third aliquot of beads was added, and the shaker was moved to a 4°C room where the samples were shaken overnight (12-14 h). The next day, two more aliquots of beads were added and incubated for two hours at room temperature, and after the fifth incubation period the samples were lifted from the beads via pipette.

3.4. DETERGENT ADDITION STUDIES

A series of nine samples were prepared, containing equimolar liposome particles but with Triton X-100 concentrations ranging from 0 mM to 2.500 mM (Table 2). Samples were incubated in a water bath at temperature (20 °C, 50 °C, or 60 °C) for 30 min before being transferred to polystyrene cuvettes for DLS measurements at room temperature. A series of lipid-free control samples were also prepared and treated identically, containing equimolar Triton X-100 concentrations ranging from 0 mM to 2.500 mM in EBSS without liposomes.

Table 2. Triton X-100 treatment concentrations and corresponding treatment ratios (R_T) for detergent-addition studies.

Triton X-100 Concentration*		Total Lipid Concentration**	Molar Treatment Ratio
mM	µg/mL	µM	R_T (Triton X-100/Lipid)
0	0		/
0.062	39.00		1.14
0.125	78.00		2.29
0.250	156.44		4.59
0.500	312.44	54.5	9.17
0.750	468.81		13.8
1.000	624.81		18.3
1.250	781.25		22.9
2.500	1562.44		45.9

* Triton X-100 concentrations apply to both the liposome – Triton X-100 mixtures and the buffer- Triton X-100 control mixtures.
** Lipid concentration as calculated before extrusion.

3.5. DETERGENT REMOVAL STUDIES

Liposome samples were prepared with final Triton X-100 concentrations of 0 mM, 0.125 mM, 0.250 mM, and 0.500 mM (see Table 3 below).

Samples were incubated at temperature (20 °C, 50 °C, or 60 °C) for 30 min and 500 µL aliquots of each sample were then treated with 5 consecutive incubations with 3 mg of beads. The first two incubations were performed for two hours at 20 °C, followed by an overnight incubation at 4°C, and two more two hour 20 °C incubations the next day. At the time of each addition, 2-3 µL of each sample was removed for Nanodrop UV-Vis absorption measurement. The remainder of the Triton X-100 treated samples were shaken along with the Bio-Bead-treated samples but were not otherwise perturbed. After the 5 incubation periods, all samples were removed from Bio-Beads.

Table 3. Triton X-100 treatment ratios (R_T) and corresponding Triton X-100 and lipid concentrations for detergent-removal studies.

Treatment Ratio of Triton X-100 to Lipid		Triton X-100 Concentration	Lipid Concentration *
Label	R_T	mM	µM
i	1.72	0.125	
ii	3.44	0.250	72.7
iii	6.88	0.500	

*Lipid concentration as calculated before extrusion.

For Figure 3 data, absorbance at 280 nm of the 2-3 µL aliquots of only untreated, Triton X-100-saturated liposomes (labeled TX), and 5x Bio-Bead-treated Triton X-100-saturated liposomes (labeled TX +BB) was measured. For Figure 4 data, absorbance at 280 nm of the 2-3 µL aliquots of Triton X-100-saturated liposomes (labeled 0 mg Bio-Beads), and each of the 5 consecutive Bio-Bead-treated Triton X-100-saturated liposome samples (5, 10, 15, 20, 25 mg Bio-Beads) was measured.

3.6. RECONSTITUTION STUDIES

For the spike protein reconstitution experiments, a previously reported detergent-mediated reconstitution method was adapted[33,36]. For "protein reconstitution" samples, tenfold diluted liposomes (1x liposomes) saturated with 0.250 mM Triton X-100 (R_T ii) were supplemented with 25 nM Spike-LMNG-AF633. (Final concentrations shown in Supplementary Table S2). The sample was incubated at 20 °C for 90 min. The sample was then treated with 5 consecutive incubations with 3 mg of beads. As above, the first two incubations were performed for two hours at 20 °C, followed by an overnight incubation at 4°C, and two more two hour 20 °C incubations the next day. After the 5 incubation periods, all samples were removed from the beads. For "dye reconstitution" samples, tenfold diluted liposomes (1x liposomes) saturated with 0.250 mM Triton X-100 (R_T ii) were treated with AF633 in ddH_2O at a concentration calculated using the following formula:

$$[AF633] = n \cdot [Spike - LMNG - AF633] \quad (1)$$

Where n represents the degree of labeling of the protein (number of dye molecules per molecule of protein). These samples were otherwise treated identically to the protein samples. "Mock reconstitution" samples were tenfold diluted liposomes (1x liposomes) saturated with 0.250 mM Triton X-100, treated with an equal volume of EBSS as was added protein and dye in the "protein reconstitution" and "dye reconstitution" samples, respectively, and the samples were treated identically otherwise. "Liposome" samples were simply diluted with EBSS (no Triton X-100) but temperature-treated along with the other samples. No Bio-Beads were added to the "liposome" samples, but they were incubated at temperature along with the Bio-Bead-treated samples.

3.7. DYNAMIC LIGHT SCATTERING (DLS)

Dynamic light scattering (DLS) experiments were performed using Malvern Panalytical Zetasizer Advance Series – Ultra (Red Label) instrument to measure the diameter and polydispersity index (PDI) of the nanoparticles. Settings included a backscatter measurement angle of 173° and a 633nm incident laser wavelength for the 4.0 mW He-Ne laser. Measurements were performed within 10 mm path length polystyrene cuvettes in minimum triplicate.

3.8. NANODROP UV-Vis SPECTROPHOTOMETRY

All Nanodrop extinction measurements were conducted using a Thermo Fisher Scientific NanoDrop 2000/2000c spectrophotometer with a 1 mm pathlength. All measurements were conducted in minimum triplicate.

3.9. FLUORESCENCE CORRELATION SPECTROSCOPY

3.9.1. Two-Photon Excitation Fluorescence Correlation Spectroscopy (TPE-FCS)

Two-photon excitation fluorescence correlation (TPE-FCS, hereafter "FCS") was used to monitor

and verify protein reconstitution. Two-photon excitation was used because its femtolitre-range interrogation volume improves detection of fluctuations in fluorescence and reduces thermal and photo-damage to the sample. FCS allows fluctuations of fluorescence intensity within a given interrogation volume to be monitored over time. Importantly, this is done in a non-invasive manner that does not affect the equilibrium of the system.

3.10. TPE-FCS AUTOCORRELATION ANALYSIS:

By analyzing autocorrelation data from one fluorophore, FCS provides information on changes in relative concentrations of the fluorophore, which can give indirect information about processes such as binding, aggregation, fluorescent quenching, or energy transfer. Diffusion coefficients can also be obtained from the data which can inform about the size of the diffusing entity. During an FCS measurement, molecules diffuse in and out of the excitation volume due to Brownian motion, and their fluorescence is detected when inside the TPE volume. The count rate trajectory describes the average fluorescence intensity per time window, from the fluorescence emitters within the TPE volume. As this fluorescence intensity fluctuates over time, the signal is autocorrelated temporally to show the self-similarity of the signal as a function of lag time, τ. Physically, this autocorrelation decay represents the likelihood of finding the same emitter particle within the TPE volume at different lag times. The normalized autocorrelation trace can be fitted using the following function:

$$G(\tau) = G(0) \cdot \left(1 + \frac{8D\tau}{{r_0}^2}\right)^{-1} \cdot \left(1 + \frac{8D\tau}{{z_0}^2}\right)^{-\frac{1}{2}} \quad (2)$$

where r_0 is the laser beam waist radius, τ is the lag time, D is the diffusion coefficient, and z_0 is the excitation focal volume depth. The autocorrelation amplitude, G(0), is influenced by brightness (η) and molar concentration (C) of emitters as shown in the expression below, where N_A is Avogadro's number and V is the TPE focal volume.

$$G(0) = \frac{\Sigma_i \eta_i{}^2 C_i}{(\Sigma_i \eta_i C_i)^2 \cdot V \cdot N_A} \quad (3)$$

Assuming one 'type' of emitting fluorophore (i.e., uniformity of fluorescent brightness and diffusive properties of the particles in solution), and accounting for the calibrated focal volume, equation 3 can be simplified to equation 4 below:

$$G(0) = \frac{1}{N} \quad (4)$$

where N represents the average number of fluorescent particles inside the focal volume. The brightness per particle can then be approximated by dividing the total fluorescence within the focal volume by the number of particles within that volume, as shown in equation 3.4.

$$\eta = \frac{<F>}{N} = < F > \cdot\ G(0) \quad (5)$$

3.11. TPE-FCS/FCCS INSTRUMENTATION

A mode-locked Titanium:Sapphire 100 fs pulsed laser, operating at a 82 MHz repetition rate, with an excitation wavelength of 774 nm was used for all TPE-FCS experiments. In the chosen optical arrangement, a sequence of mirrors and lenses direct and expand the excitation laser beam to fill the back aperture of a 40X, 1.2 NA, 0.8 mm working distance water-immersion objective lens. This objective lens collects fluorescence emissions of the diffusing particles in the TPE volume and reflects this emitted light to a dichroic optic which separates it from the excitation light. The fluorescence is then further separated into the two distinct colored light paths and finally each is passed through a spectral notch filter and directed to a separate avalanche photodiode detector. The fluorescence intensity information from the photodiodes is analyzed by a PC using a correlator card (ALV-6000), and plotted and processed using OriginPro 2019 software.

3.12. STATISTICAL ANALYSIS

Pairwise comparisons were executed via two-tailed t-tests assuming equal variance. Multi-level comparisons or multi-factor comparisons were carried out using one- or two-way ANOVA respectively. All statistical analysis was performed using number of independent experiments as number of replicates (n=3), despite technical replicates (n>3) also being

plotted in figures. Number of replicates and level of significance is indicated for each result. Statistical tables are found in Supplementary Tables 3.5-3.10.

4. Results

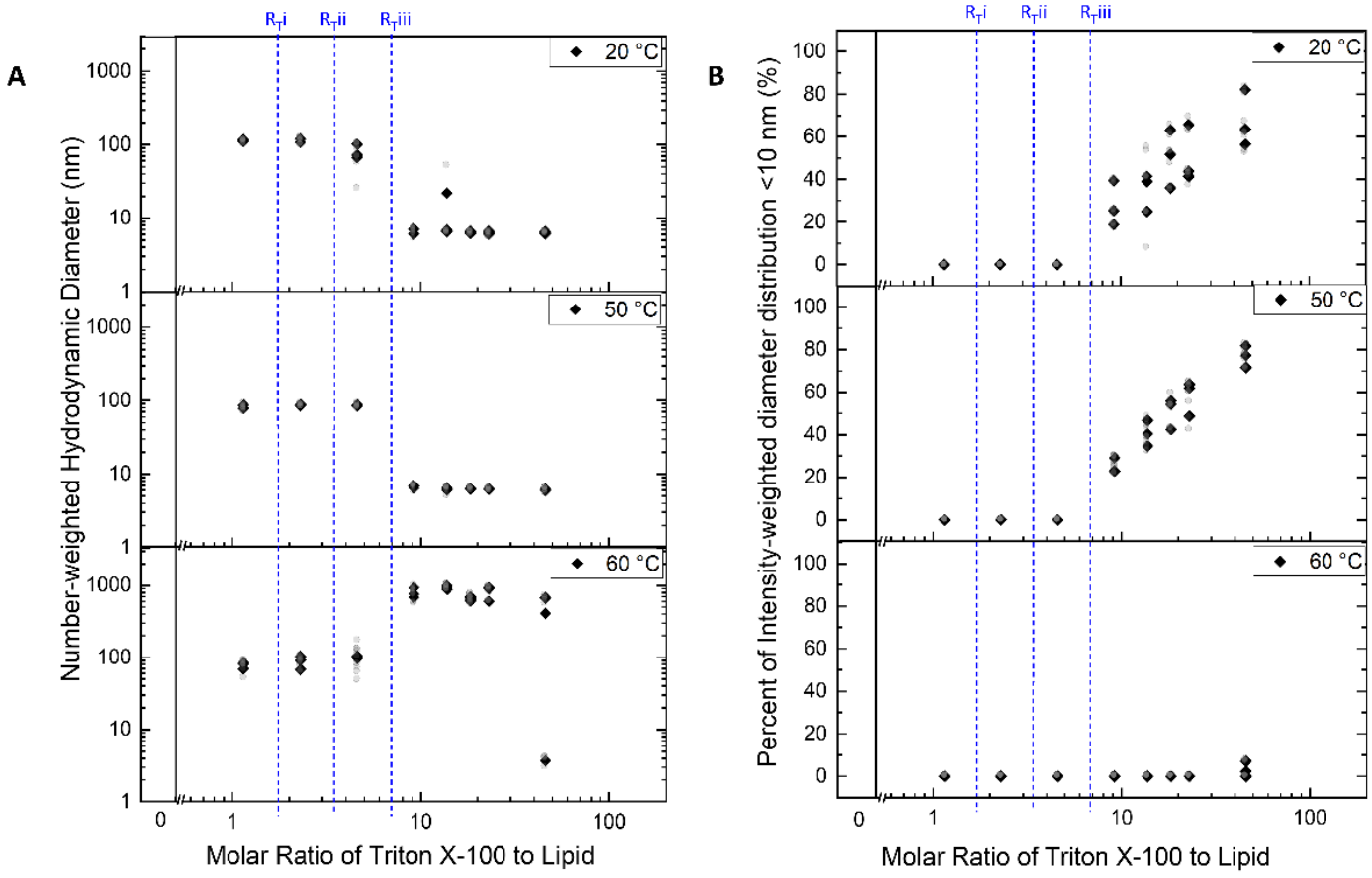

Figure 2. A) Number-weighted hydrodynamic diameter data for liposomes treated for 30 min at 20 °C, 50 °C, or 60 °C with increasing relative concentrations of Triton X-100. B) Percent of the intensity-weighted hydrodynamic diameter distribution that is under 10 nm in diameter for liposomes treated for 30 min at 20 °C, 50 °C, or 60 °C with increasing relative concentrations of Triton X-100. For both A and B, black diamonds represent biological replicates and grey circles represent technical replicates. Blue lines labeled i, ii, and iii represent Triton X-100 to lipid ratios relevant for comparison with Figure 3 and 4.

4.1. DETERGENT ADDITION STUDIES

To determine the saturation points of liposomes at different temperatures, solutions of liposomes treated with Triton X-100 at different Triton X-100 to lipid treatment ratios (R_T) were analyzed using DLS. Under all temperature conditions, as liposomes were treated with increasing concentrations of Triton X-100, the number-weighted diameter remained relatively constant until an approximate R_T of 4.6 after which point the behaviour of the solution differed notably depending on the temperature (Figure 2A). For 20 °C and 50 °C treatment conditions, the number-weighted diameter distribution of the solutions remained monomodal but dropped by an order of magnitude to a diameter range of 5-8 nm after the R_T surpassed 4.6. In contrast, the number-weighted diameters reported for the liposome solutions treated with Triton X-100 at 60 °C increased to over 600 nm above this R_T. When examining solutions of Triton X-100 without liposomes present (henceforth, Triton X-100 controls), the number-weighted hydrodynamic diameter (HD) values of the control produced at 60 °C does not fall into the size range of a typical micelle (<10 nm) until 1.3 mM Triton X-100,

compared to the controls at 20 °C and 50 °C which fall into this range once the Triton X-100 concentration reaches 0.5 mM (Supplementary Figure S1A,B).

Another way of looking at these population changes was to examine the intensity-weighted HD distributions (which were often multimodal) and quantify the percent of the overall distribution that fell in the size range of a typical micelle (<10 nm)[38]. For both 20 °C and 50 °C conditions, micelle-sized species began to appear in measurable proportions at treatment ratios above R_T = 4.6 (Figure 2B). The proportion of micelle-sized species in solution continues to increase linearly with increased Triton X-100 after this R_T. At 60 °C saturation conditions, however, micelle-sized entities were not observed until an R_T of 46 was reached, representing an order of magnitude higher Triton X-100 concentration (Figure 2B, bottom panel). Even at this point, however, these micelles were observed only minimally (<15% of distribution). Looking at the intensity-weighted diameter distributions, Triton X-100 controls prepared at 60 °C developed micelle-sized populations above 1.0 mM Triton X-100 which is a markedly lower concentration threshold than the 2.5 mM which was required to observe micelle-range entities when liposomes were present (Supplementary Figure S1C, D). Still, however, the Triton X-100 controls prepared at 60 °C required more Triton X-100 to show micelle-sized species formation compared to those controls prepared at 20 °C or 50 °C (Supplementary Figure S1D).

4.2. DETERGENT REMOVAL STUDIES

Because liposomes show minimal absorbance at 280 nm and the phenyl moiety of Triton X-100 has a 280 nm absorbance maximum, monitoring changes in 280 nm absorbance can provide insight into the quantity of Triton X-100 in a detergent-treated liposome system[39]. Absorbance at 280 nm was measured for solutions of untreated liposomes as well as liposomes with Triton X-100 added at R_T values i = 1.7, ii = 3.4, and iii = 6.9 (0.125 mM, 0.250 mM, and 0.500 mM Triton X-100, respectively) treated at 20 °C, 50 °C, or 60 °C. 280 nm absorbance was compared before and after Bio-Bead treatment to verify the removal of Triton X-100 from solution. For all concentrations of Triton X-100 and all temperatures (except R_T i at 50 °C), the 280 nm absorbance was significantly reduced after Bio-Bead treatment (Figure 3). Moreover, except for R_T i at 50 °C, all liposome treatments showed a final post-Bio-Bead 280 nm absorbance that was not significantly different than the initial pre-Triton X-100 sample.

Absorbance at 280 nm was also compared across three saturation temperatures for each concentration of Triton X-100 in the treated liposomes to determine if the temperature of saturation influenced the absorbance reading for that detergent concentration (Supplementary Figure S2A). For R_T i (corresponding to 0.125 mM Triton X-100), absorbance at 60 °C was significantly higher than that at 20°C and 50°C. For R_T ii (corresponding to 0.250 mM Triton X-100), absorbance at 60 °C was significantly higher than 50 °C, however there was no significant difference between the 20 °C saturated sample absorbance and the other temperatures. Notably, for R_T iii (0.500 mM Triton X-100), there was no significant difference between absorbance at 280 nm for any of the three saturation temperatures.

For all three concentrations of Triton X-100 used to saturate liposomes at 20 °C, when absorbance at 280 nm was measured after each sequential treatment of the liposomes with Bio-Beads, the only significant decrease in absorbance was observed after the first addition of beads (Figure 4A, 4D, 4G). For the four subsequent additions, no significant difference was observed in the sample absorbance. The same was largely observed for the samples saturated at 50°C and 60 °C (Figure 4E,F,H,I), however for the lowest Triton X-100 concentrations at these temperatures there was no significant difference in absorbance measured at any point in the Bio-Bead addition process (Figure 4B, C). Notably, similarly to the trend seen in Figure 2, samples saturated at 60 °C showed a higher absorbance at all steps in the Triton X-100 removal process and had a greater variability in the data.

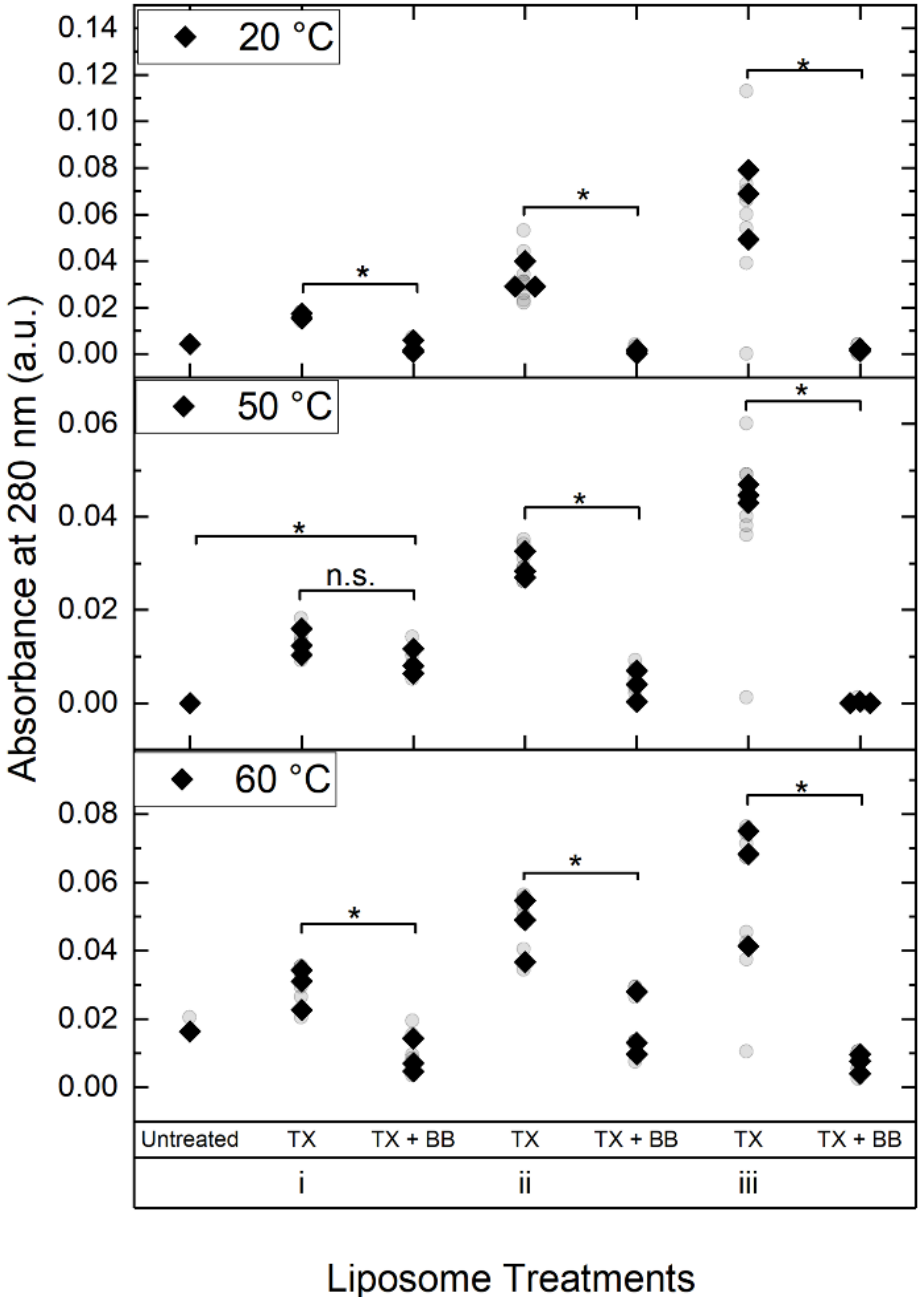

Figure 3. Absorbance at 280 nm for liposome samples treated at 20 °C, 50 °C, or 60 °C with Triton X-100 at R_T values of i = 1.7, ii = 3.4, and iii = 6.9, before (TX) and after (TX + BB) detergent removal using BioBeads. Two-sample t-tests were used to compare absorbance values before and after BioBead treatment, as well as to compare post-BioBead absorbance for each tested concentration with the absorbance of the untreated sample. Grey circles represent technical replicate measurements of all independent experiments and black diamonds represent the mean of the technical replicate measurements for each individual experiment ('biological' replicates).

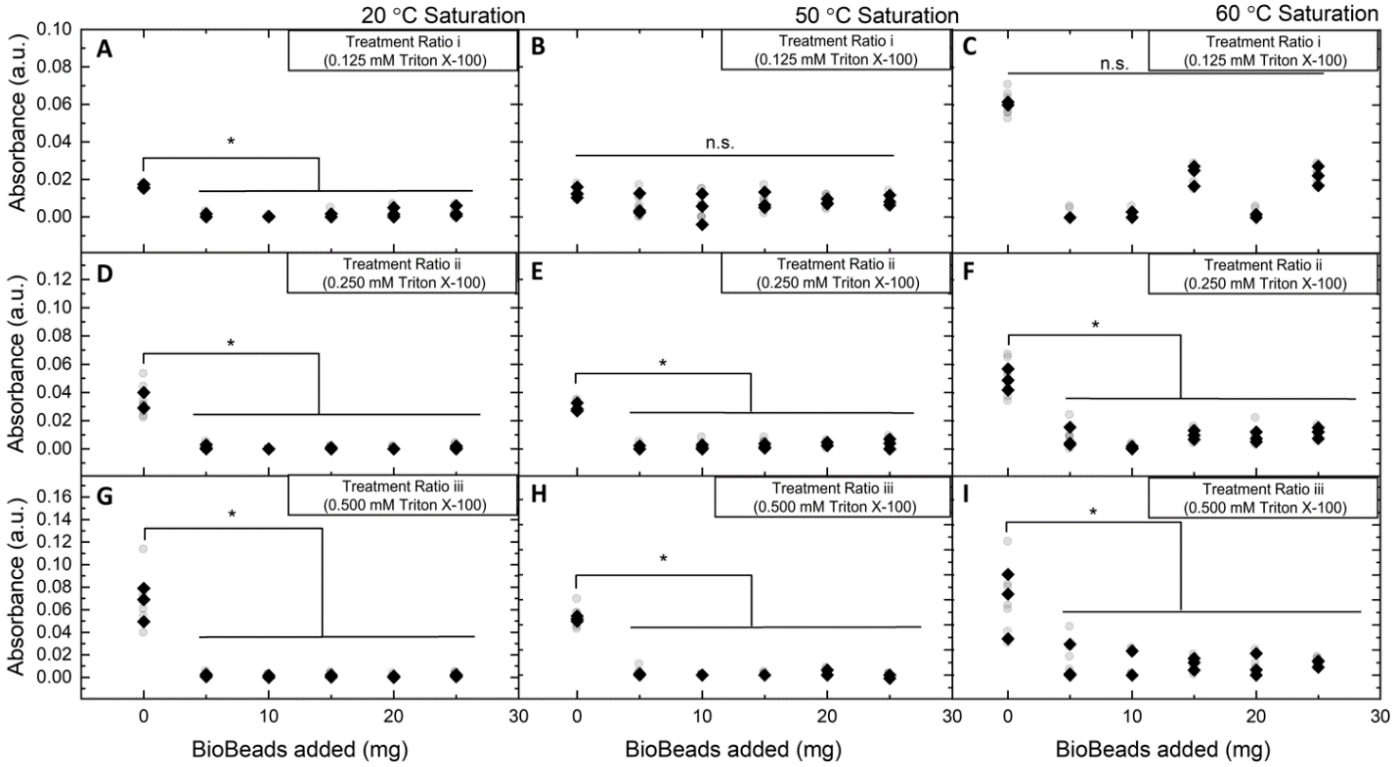

Figure 4. Absorbance at 280 nm for liposome samples treated at 20 °C, 50 °C, or 60 °C with 0.125, 0.250, or 0.500 mM Triton X-100 at the point of saturation (0 mg BioBeads) and after each subsequent 5 mg BioBead addition. Black diamonds represent biological replicates and grey circles represent technical replicates. Statistical significance was tested using one-way ANOVA and Tukey's post-hoc test, and significance is denoted by * ($p < 0.05$). Grey circles represent technical replicate measurements of all independent experiments and black diamonds represent the mean of the technical replicate measurements for each individual experiment ('biological' replicates).

4.3. DETERGENT-MEDIATED RECONSTITUTION STUDIES

The effect of saturation temperature on SARS-CoV-2 Spike Glycoprotein reconstitution into liposomes was first explored using DLS to analyze resulting particle diameter after reconstitution. From previous work, we expected to see a slight diameter increase upon reconstitution of proteins into liposomes, likely due primarily to the extra size of the extravesicular portion of the membrane proteins inserted[36]. Here, however we were interested in probing the effect of detergent saturation temperature on the particle properties. 2-way ANOVA analysis of the data revealed a significantly higher Z-average HD for all samples saturated at 50 °C and 60 °C compared to those saturated at 20 °C (Figure 5A). Moreover, generally unsaturated liposomes compared to all reconstitution attempts showed a significant difference in Z-average HD, but the interactions between the factors were statistically significant. This means that the difference between the Z-average HD of unsaturated liposomes and the other particles was very pronounced for the samples prepared at 50 °C and 60 °C and that difference was significantly less pronounced for the samples prepared at 20°C (Figure 5A). When examining the number-weighted and intensity-weighted data compared to this Z-average data, a similar trend is found except that the data for the 60 °C saturated particles are significantly greater than both the 20 °C and 50 °C data (Figure 5B, 5C). In addition, using these two data-weighting methods there is no significance seen when comparing the liposomes to the reconstitution samples regardless of temperature (Figure 5B,5C).

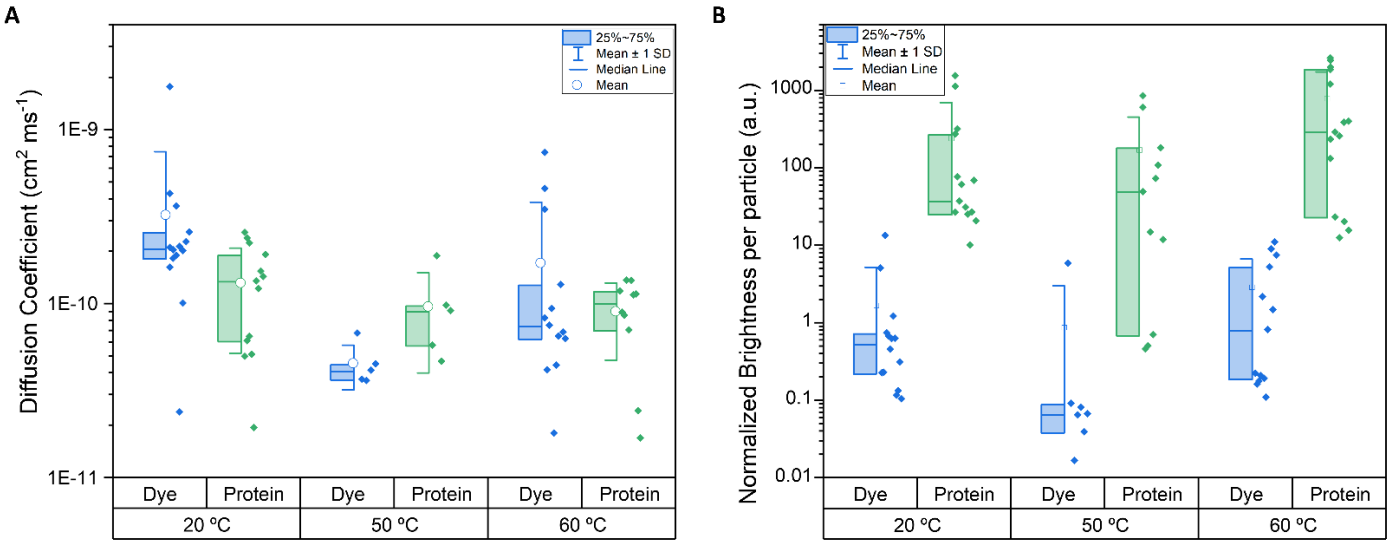

Figure 6. A) Average diffusion coefficient values, in $cm^2\ ms^{-1}$, obtained via FCS autocorrelation analysis of dye reconstituted liposomes (blue) and protein-reconstituted liposomes (green). B) Fluorescent brightness per particle, normalized to the brightness per particle of freely diffusing dye-labeled spike glycoproteins in LMNG micelles, of dye-reconstituted liposomes (blue) and protein-reconstituted liposomes (green).

Protein reconstitution into liposomes was also monitored across three Triton X-100 saturation temperatures using two FCS autocorrelation – based analyses. First, diffusion coefficients were obtained for fluorescent diffusing particles produced by reconstituting either freely diffusing AF633 or AF633-labeled SARS-CoV-2 Spike glycoproteins into liposomes by detergent-saturation at 20 °C, 50 °C, or 60 °C. (Figure 6A). Second, fluorescent brightness-per-particle measurements obtained for the fluorescent diffusing particles were compared between AF633 dye-reconstituted or spike protein-reconstituted liposomes prepared as previously mentioned (Figure 6B). The diffusion coefficient measured by FCS for the fluorescent particles in the 60 °C saturated samples was not significantly different than those for the other temperatures, and between the dye-reconstituted and protein-reconstituted particles there was also no significant difference (Figure 6A). Looking at each saturation temperature independently, while no significant differences were observed due to large data variance common to FCS analyses, there was a notably higher (approximately two orders of magnitude greater) mean brightness per particle for samples reconstituted with Spike-AF633 compared to those reconstituted with AF633 alone (Figure 6B). Between the different saturation temperatures, however, there did not seem to be a trend in the average brightness per particle for proteins or dye reconstituted into liposomes, other than a non-significant increase in median brightness of protein-reconstituted liposomes as temperature increased (Figure 6B).

5. Discussion

Hydrodynamic Diameter distribution changes of liposomes treated with Triton X-100 monitors detergent saturation of liposomes.

Liposome saturation point was determined by monitoring the HD distribution of solutions of liposomes as Triton X-100 was added, noting the R_T at which the system began to change. The weighting of DLS data provides different information about the system being examined, and comparing number-weighting and intensity-weighting of the same dataset can offer distinct insights into the composition of a complex solution. Number-weighting biases the HD distribution data toward the diameter of the most commonly occurring or prevalent species in solution. The number-weighted HD data here was expected to report on the R_T at which the most prevalent species in solution became micelle-sized, ostensibly due to the onset of membrane solubilization of liposomes into mixed micelles. The point directly before this onset of solubilization represents the

"saturation ratio" (R_{SAT}) for this liposome formulation, where the maximum detergent is incorporated in and/or around the membrane before the size distribution becomes overwhelmed with micelles (either mixed micelles of membrane lipid and detergent or single component micelles of pure Triton X-100). From the data in Figure 2A, the highest tested R_T at which the number-weighted HD remains in the order of magnitude of the untreated liposomes is 4.6 when the liposomes are treated with the Triton X-100 at 20 °C or 50 °C. Based on this, the R_{SAT} of these liposomes should be somewhere between 4.6 and the next tested ratio, 9.2. Similarly, however, at these temperatures when liposomes are absent, Triton X-100 control solutions above the concentration corresponding to R_T 4.6 (0.250 mM) show number-weighted HD values in the size range expected for micelle formation. This can be explained by the fact that the critical micelle concentration (CMC) of Triton X-100, while solvent-dependent and not characterized in literature in EBSS, is likely less than or equal to its range of 0.22-0.24 mM Triton X-100 in water because of the presence of salts in the EBSS solution[40,41]. Therefore, based on this data alone it is impossible to conclude that the change in number-weighted diameter in the Triton X-100-treated liposome samples in Figure 2A is due exclusively to solubilization of the liposomes into micelles, but likely a combination of solubilization into mixed micelles and production of pure Triton X-100 micelles is occurring. In contrast to the number-weighted data analysis, intensity-weighted DLS data represents the "rawest" form of the data that, while biased towards species which most scatter light (i.e., larger particles), can still be useful to evaluate the populations of species within a solution and their relative proportions. We represented the formation of micelles by plotting the percentage of the total distribution that fell into the <10 nm diameter range. Thus, the appearance of species within the micellar size range in the intensity-weighted distribution after an R_T of 4.6 supports the conclusion from the number-weighted data that this R_T could be the effective saturation point for the liposome system here. When examining Triton X-100 – treated liposome solutions and comparing them to Triton X-100 controls, the latter showed a higher degree of micelle evolution than the former at almost every equivalent Triton X-100 concentration (Supplementary Figure 2C,D). This again suggests that the presence of liposomes in the solution suppresses initial micelle formation, perhaps because Triton X-100 incorporation into the liposome membranes reduces the effective concentration of Triton X-100 in the solution.

5.1. R_{SAT} OF MULTI-COMPONENT LIPOSOMES IS INFLUENCED BY INTERDEPENDENT FACTORS

Saturation of liposomes by Triton X-100 and other surfactants is very dependent on liposome composition and is clearly related to elements of membrane structure such as headgroup electrostatics, lipid tail interactions and resulting membrane fluidity, sterol presence, and lipid shape factor. Several theories exist as to the mechanism of these detergent – membrane interactions and which factors are most influential for such processes. The liposome formulation in the present study contained 77.5% sub-zero melting temperature lipids (T_m< 0 °C) and less than 15% lipids with T_m above 20 °C (See Table 1), meaning that at 20 °C, 50 °C, or 60 °C the membranes were likely predominantly fluid with some ordered regions. The cholesterol present in the formulation, however, probably conferred an additional degree of order to the membranes, since cholesterol has been shown in literature to both promote the formation of liquid ordered (l_o) regions with saturated lipids as well as liquid disordered (l_d) regions with unsaturated lipids[42,43]. Cholesterol has long been reported as a key player in detergent-resistant membranes (DRMs), often in concert with sphingolipids but also associated with saturated glycerophospholipids such as the those found in the presently investigated membrane formulation[44]. A theory by Arnulphi et al. states that the mechanism of Triton X-100 partitioning must be different for gel vs fluid membranes because the free energy of partitioning is the same for these two systems, but gel-phase lipids become saturated at lower detergent concentrations[45]. Regardless of mechanism, strong

bodies of evidence exist in literature suggesting that membrane fluidity has a very strong influence on the concentration of detergent required to saturate a liposome, typically fluid-phase membranes requiring more detergent to become saturated than those in the gel or l_0-phases[45,46].

When comparing the R_{SAT} range reported here of 4.6 – 9.2 moles Triton X-100 per mole lipid to other fluid-phase systems with similar headgroup proportions in literature, we observe that the liposomes here are saturated at R_T values which are substantially greater than those found for relevant systems in literature. For example, a study by López *et al.,* reported a Triton X-100 R_{SAT} between 0.63-0.94 for PC-based liposomes derived from egg lecithin[47]. Another study by Patra et al. investigating pure DOPC liposomes reported a ratio of moles Triton X-100 per mole of DOPC required to solubilize 50% of the liposomes (R_{SOL50}) of 1.93, which should be a higher ratio than the true R_{SAT} for such a system[46]. Because egg-PC and DOPC membranes are more fluid at room temperature than those investigated here, it would follow based on the Lichtenberg and Arnulphi models that these fluid membranes would require more detergent to saturate than those presently investigated, but the opposite is in fact observed. Other published data seems to disagree with the premise that gel-phase membranes require less detergent to saturate or solubilize. Some voices have proposed that more ordered bilayers pose a kinetic challenge for partitioning of Triton X-100, and that adding more detergent and increasing the collision frequency between Triton X-100 molecules and the membrane surface could be necessary for saturating or solubilizing such gel-phase membranes[46]. The kinetic challenge of gel-phase membranes and their interactions with detergents is echoed by Lichtenberg and coworkers, and as such a balance of thermodynamic and kinetic arguments is obviously at play when discussing these relationships[48]. That said, a study examining entirely gel-phase PC liposomes composed of either DPPC and DSPC reported R_{SOL50} values of 1.7 and > 5 respectively at room temperature[46]. Since the liposomes we are investigating here have far lower proportions of gel-phase lipids at room temperature and yet a higher amount of Triton X-100 required to be saturated, this kinetic argument cannot fully explain what is observed.

If phase cannot fully explain the high R_{SAT} observed for the present liposomes, perhaps a combination of phase effects and physicochemical headgroup-detergent interactions can help to understand. The liposomes studied here were primarily composed of PC headgroups (77.5%), with small proportions of PE (8.7%) and PI (4.6%) (Table 1). The presence of PE within a membrane has been shown to prevent the solubilization of liposomes and as such could possibly explain the extra Triton X-100 required to saturate the particles prepared in this current study which have a composition of 8.7% PE[49]. For example, liposomes comprised of *Escherichia coli* crude membrane extract which are highly enriched in PE have been reported to have an approximate R_{SAT} ~ 3 for Triton X-100[33]. This effect is shown to be dependent on the proportion of PE within a membrane, however, and studies have shown that 9% PE in PC-dominant membranes behave very similarly to pure PC liposomes[49]. In addition, PE-cholesterol interactions that have been reported to lead to detergent-resistant lipid raft formation in the inner leaflets of model membranes have exclusively been observed for PE lipids with at least one unsaturated acyl chain, and not observed for the fully saturated DPPE used in this present study[50]. Despite this, the presence of DPPI alongside the DPPE in the membranes studied here, especially with the coexistence of cholesterol in the membrane, might produce a combinatorial effect in terms of detergent resistance. This suggestion is supported by evidence of detergent-resistant membrane (DRM) localization and enrichment of phosphoinositide lipids *in vivo*[44,51], although this depends strongly on lipid saturation, cell type, and the physiological state of cell signaling pathways as some reports suggest depletion of PIs within DRMs[51,52]. In the present work, however, the presence of divalent calcium cations in EBSS (see Supplementary Table S3) neutralizing

the negative headgroup charge of PI likely contributes to the ordering of DPPI lipids in the liposome membranes which could contribute to the formation and stabilization of localized PI-enriched DRM regions within the liposomes[53].

5.2. LIPOSOME SATURATION POINT (R_{SAT}) DETERMINATION REVEALS LITTLE INFLUENCE OF SATURATION TEMPERATURE

The detergent saturation of liposomes exposed to Triton X-100 was monitored at different temperatures to report on the whether elevated temperatures would influence the interactions between Triton X-100 and liposomes. We observe in the present study that the R_{SAT} range for the liposomes does not seem to change with the increase in saturation temperature from 20 °C to 50 °C (Figure 2 top, middle). While the range of R_{SAT} of 4.6 – 9.2 reported by the DLS data here makes resolving slight changes in R_{SAT} as a function of temperature impossible, certainly dramatic changes in R_{SAT} are not occurring. Generally, this suggests that the entropic contribution to the free energy of the detergent insertion may not be strong, given that changing the temperature does not notably change the R_{SAT}. This partially agrees with literature studies in which liquid crystalline DOPC liposomes do not experience a change in R_{SAT} with elevated saturation temperatures. The effect of temperature on saturation of liposome membranes with Triton X-100 has been explored in literature, particularly as it pertains to the change in membrane fluidity that occurs when the melting temperature of a lipid substituent is surpassed[46]. Although based on work by Patra and coworkers we might expect to see a decrease in overall R_{SAT} due to the melting transition of DPPI above its 41 °C transition temperature, likely the low proportion of DPPI within the membrane prevents such an effect from dominating the liposome behaviour[46]. In addition, the presence of Ca^{2+} discussed earlier likely increases the melting temperature of such regions by reducing intermolecular repulsion between phosphate-inositol headgroups[53].

5.3. SATURATION OF LIPOSOMES ABOVE THE CLOUD POINT OF TRITON X-100 LEADS TO THE FORMATION OF MICRON-SIZED LIPID-DETERGENT AGGREGATES

When liposomes are treated with Triton X-100 at 60 °C, however, the resulting number-weighted HD distributions are dominated by micron-scale particles after R_T 4.6, which suggests aggregation of Triton X-100 and/or formation of lipid-detergent aggregates. The same is seen initially in the 60 °C Triton X-100 control (Supplementary Figure S1B). This aligns with research performed previously in which surpassing the cloud point of Triton X-100 leads to formation of aggregates containing up to 10^{10} molecules with an overall HD up to 3 µm[54]. The cloud point of Triton X-100 is the temperature above which a solution of micelles splits into two phases, one so-called coacervate phase highly enriched in surfactant aggregates that exclude water, and another aqueous phase containing detergent at or near the critical micelle concentration[55]. The cloud point of Triton X-100 in pure water is 65 °C, but this temperature decreases with the addition of metal salts such as NaCl and KCl[55]. It follows, then, that for Triton X-100 / liposome solutions in EBSS, which contain metal ions in mM quantities (see Supplementary Table S3), depression of the cloud point may be responsible for the observed large aggregates forming under 60 °C conditions for Triton X-100 controls as well as detergent-treated liposomes. Notably, however, in the present study the number-weighted diameter distribution of the Triton X-100 control drops to being micelle-size dominant above 1 mM Triton X-100 (Supplementary Figure S1B). A similar phenomenon was observed in literature where Triton X-100 aggregates maintained at elevated (above cloud point) temperature began to decompose into 7-15 nm particles, and this was explained by suggesting that such aggregates break due to thermal motion[54]. The fact that in the current study this aggregate breakdown is not seen in the liposome-containing samples except in one replicate at the highest R_T corresponding to 2.5 mM Triton X-100 (Figure 2A, Supplementary Figure S1A) suggests that the presence of liposomes changes the behaviour

and perhaps composition of aggregates at 60 °C[56,57]. The minimal formation of micelles in liposome solutions treated with Triton X-100 at 60 °C agrees with the theory from the number-weighted analysis above that large micron-scale aggregates are being produced under these conditions and we propose here that these contain liposome aggregates as well (Supplementary Figure S2A,C).

5.4. REMOVAL OF SATURATING TRITON X-100 FROM LIPOSOME SOLUTIONS DOES NOT DEPEND ON TEMPERATURE

Determining the extent of detergent removal during protein reconstitution is essential, as leftover detergents can interfere with the structure and function of proteoliposomes and can interfere with target cell membranes if left in solution. Typical dialysis methods of detergent removal are not highly effective for detergents with low CMC values such as Triton X-100, since the micelle size is larger than allowed by filtration membrane exclusion limits, and dilution effects can be detrimental to the experimental goals[57]. Better, then, is the use of non-polar adsorbent materials such as Bio-Beads, but the effectiveness of this adsorption process depends on the binding capacity of these beads (specific to the physicochemical structures of the detergents being removed), the availability of un-bound bead surface to the detergent, the temperature of detergent removal, and the degree to which other species compete with detergent for bead binding[57]. Therefore, the Triton X-100 removal assay described here was used to determine the success of this process for the specific liposome formulation and protein under investigation.

Triton X-100, while used ubiquitously in biochemistry and molecular biology, has not been extensively studied in biocompatible buffer systems and its extinction coefficient is not well-established in solvents other than methanol[39]. Because of the 280 nm absorbance of the phenyl group in Triton X-100, however, the absorbance of liposome samples treated with Triton X-100 was expected to depend linearly on the concentration of Triton X-100 present in solution for the concentrations of TX100 employed. As such, in this section of this study absorbance was used as a reporting parameter on the Triton X-100 concentration within liposome samples before detergent addition, after detergent addition, and after Bio-Bead treatment. In the detergent removal studies, three saturation conditions were selected based on the detergent addition studies (Figure 2). These conditions were selected as estimates for (i) sub-saturating conditions, (ii) saturating conditions, and (iii) super-saturating and/or solubilizing conditions. The aim of this was to develop an assay to monitor whether Triton X-100 at various concentrations could be fully removed from liposome solutions by Bio-Bead treatment. A lack of significant difference between the final post-Bio-Bead absorbance and the initial untreated liposome sample absorbance for all but one of the experimental conditions suggests that the Triton X-100 was fully removed from the solution. The one significant difference between untreated and Bio-Bead-treated liposome absorbance (R_T i, 50 °C) may have been due to the challenges of adding precise and replicable quantities of Bio-Beads to the samples given their high size polydispersity.

To verify the assumption used in this assay of a linear relationship of 280 nm absorbance to Triton X-100 concentration, absorbance values for the four Triton X-100 concentrations corresponding to untreated liposomes and R_T i, R_T ii, and R_T iii were plotted and linear fit functions were applied (Supplementary Figure 1B, red fit lines). For samples prepared at 20 °C and 50 °C, the absorbance data showed a linear concentration dependence with equal slopes and R^2 values over 0.98. (Supplementary Figure S1B, top and middle). This suggests that 280 nm absorbance of its phenyl moiety can be a reasonable proxy for Triton X-100 concentration under these conditions. For samples prepared at 60 °C, however, while the absorbance data can be fitted with a linear function with a similar slope to the two lower temperature datasets, the lower R^2 value of 0.93 and the appearance of the data as beginning to plateau in absorbance after 0.250 mM Triton X-100 suggests that there is a saturation

of signal response after this point (Supplementary Figure S1, Bottom). As such, all three plots were re-fitted omitting the 0.500 mM Triton X-100 data (Supplementary Figure S1, blue fit lines). While the slopes and R^2 values of the 20 °C and 50 °C truncated fit lines were only slightly greater than those from the full-dataset fit lines, the fit line of the truncated 60 °C data had a slope of 0.16 and R^2 value of 0.96, indicating that this steeper slope better fit the lower-concentration datapoints and that some saturation of signal was occurring at this temperature.

To further understand the relationship between Triton X-100 concentration in the liposome solutions and the resulting 280 nm absorbance, the absorbance of each concentration of Triton X-100 in treated liposome samples was compared across each of the three temperatures (Supplementary Figure S2A). The significant difference observed in absorbance between 50 °C and 60 °C treated samples in the two lower-concentration conditions reflects a similar phenomenon as did the difference in slope at elevated temperatures and lower Triton X-100 concentrations (Supplementary Figure S2B, blue fit lines). Based on these data, significant changes are apparent when comparing the optical properties of liposome samples treated with Triton X-100 at 50 °C with those treated at 60 °C. This can be explained by recalling that the absorbance measured by a spectrophotometer is in fact extinction, which is the sum of absorbance of a solution and the light scattering caused by the solution. At 60 °C saturation, the cloud point of the Triton X-100 is surpassed which leads to an increase in light scattering based on the previously mentioned phase separation and aggregate[54]. The fact that this is observed as a significant increase in apparent absorbance at 0.125 mM Triton X-100 (R_T i) and 0.250 mM Triton X-100 (R_T ii) but not at 0.500 mM Triton X-100 (R_T iii) suggests that at these lower Triton X-100 concentrations the absorbance term is outweighed by the light scattering term. Thus, it is challenging to use light-scattering techniques to analyze Triton X-100 solutions at elevated temperatures beyond the cloud point, however since the assay for detergent removal developed here falls within the linear range of the absorbance to concentration relationship, the data remains reliable.

5.5. BIO-BEADS REMOVE ALL MEASURABLE TRITON X-100 FROM LIPOSOME SOLUTIONS AFTER ONE ADDITION

An extension of the absorbance assay was used to monitor the stepwise removal of Triton X-100 by Bio-Beads (Figure 4). Stepwise additions have been reported to facilitate the slow removal of Triton X-100 from a solution, rendering the system more amenable for thermodynamically favourable protein insertion during detergent-mediated protein reconstitution, and the protocol used here was modified from one reported in the reconstitution of NorA-GFP[33]. As previously mentioned, however, the interactions between polystyrene adsorbents and detergents are influenced by elements of the system including ionic strength, binding surface availability, and presence and characteristics of potential competitor molecules such as membrane proteins and lipids. Therefore, while literature values are useful as a starting point to determine bead:detergent proportions for optimal removal of detergents for protein reconstitution, each individual system must be evaluated carefully and independently. Simeonov and coworkers found that 5 additions of 4-6 beads per addition was optimal to remove 300 nanomoles of Triton X-100 from solution[33], and a seminal review by Rigaud et al. in 1998 described the maximum adsorption capacity of Bio-Beads for Triton X-100 as 185 mg of detergent per g of beads[58]. In the present study, 5 additions of approximately 3 mg of beads (approximately 8-12 beads) per addition was used to remove Triton X-100 from treated liposomes, at detergent to bead ratios of 13, 26, and 52 mg/g for R_T i, ii, and iii respectively (Supplementary Table 4). The data in Figure 4 suggest that in general, all the measurable Triton X-100 is removed by the beads after the first addition, suggesting that the following four bead addition steps may be unnecessary. The two exceptions to this trend show a lack of significant difference across

absorbance measured after any number of bead additions, suggesting that perhaps signal to noise is a limiting factor in this assay at these concentrations of Triton X-100 (Figure 4B) or again as seen in Figure 3 and Supplementary Figures S2A-B perhaps additional turbidity from cloud-point aggregate formation is obscuring the analysis (Figure 4C). The removal of all detectable Triton X-100 as reported by absorbance at 280 nm after one bead addition suggests that for "slow" detergent-removal it might be necessary to reduce further the quantities of beads or incubation time per addition. With fewer beads per addition, however, the reproducibility naturally decreases due to the notable discrepancies in bead sizes, and further experimentation and development of more elegant detergent-removal protocols may be necessary if small sample volumes remain unavoidable. Future work should aim to more systematically understand the relationship between Bio-Bead quantity and addition frequency, Triton X-100 removal rate, and protein reconstitution.

5.6. RECONSTITUTION STUDIES CONFIRM TEMPERATURE DEPENDENCE OF PARTICLE AGGREGATION BEHAVIOUR

Based on the detergent addition studies, R_T ii (corresponding to 3.4 moles Triton X-100 per mole of lipid or 0.250 mM Triton X-100 for 0.0727 mM lipid) (Figure 2, Supplementary Table S1) was selected for reconstitution studies. This ratio of Triton X-100 to lipid was the highest tested value that could be confidently used without observing aggregation in liposomes or excess micelle production during the detergent addition studies (Figure 2). At each of the three saturation temperatures, the described Bio-Bead treatment protocol was shown to be more than sufficient for the removal of Triton X-100 from liposomes saturated at R_T ii (Figures 3 and 4). Therefore, the goal of the reconstitution studies was to characterize the particles that resulted from the detergent-mediated protein reconstitution using this R_T, at each tested saturation temperature.

Controls were also prepared, isolating different steps in the detergent mediated reconstitution protocol (liposome, mock reconstitution, dye reconstitution). This was in part to identify whether any large deviations in particle size possibly originated from these steps in the protocol. For example, "liposome" controls (Figure 5) were not detergent-saturated but were incubated similarly at the indicated temperature, to identify whether temperature elevation alone might cause changes in particle properties. "Mock reconstitution" samples (Figure 5) were prepared by saturating liposomes with Triton X-100 and removing the detergent with Bio-Beads, but not adding any protein, to determine if any changes in particle properties occurred because of the presence and subsequent removal of Triton X-100. "Dye reconstitution samples" (Figure 5,6) were prepared similarly to the "mock" samples but free AF633 dye was added to test whether possible free dye uptake into liposomes during reconstitution might conflate protein reconstitution analysis or influence particle size. Finally, the "protein reconstitution" samples (Figure 5,6) were prepared across the three saturation temperatures to reveal any temperature-dependency of the detergent-mediated protein reconstitution.

The significantly higher Z-average HD for samples prepared by saturation at 50 °C and 60 °C compared to those saturated at 20 °C and the interactions between the factors of treatment and temperature, suggest several possible insights (Figure 5A). At 50 °C and 60 °C saturation conditions, all detergent-treated samples (mock, dye, and protein reconstitutions) showed a significantly higher Z-average HD than did the "liposome" samples which had not been treated with detergent. In contrast, the 20 °C – saturated samples appeared to have little difference in Z-average diameter with or without the addition of Triton X-100. Since Z-average diameter is obtained from a cumulant fit of the DLS data which requires an assumption of monodispersity, a comparison of the polydispersity indices (PDIs) associated with these data can be informative of how appropriate that assumption is for a system. Indeed, when comparing the PDIs for the "liposome" samples to the PDIs for all the detergent-treated samples, the liposome control samples are

significantly less polydisperse at all temperatures tested (Supplementary Figure S3). This suggests that some large particle aggregates form when Triton X-100 is involved in sample preparation that contribute to the elevated Z-average diameters and PDIs here, but other data analysis is required to fully understand the system. Important to note is that all samples were incubated at temperature, including the Triton X-100 – free "liposome" controls. Therefore, temperature alone is not sufficient to change the Z-average HD of the particles, but the Z-average diameter and polydispersity of the system is influenced by the presence of Triton X-100 in combination with 50 °C and 60 °C saturation temperatures. This may be due in part to the effect of temperature on spontaneous curvature of most lipids; researchers have reported that increasing temperature leads to more negative spontaneous curvature of lipids and a membrane with increased curvature-related stress[59]. This change in spontaneous curvature at elevated temperatures may lead to an increase in the proportion of Triton X-100 added to the sample that becomes embedded in the membrane itself as the positive-curvature detergent molecule would favourably interact with such a membrane to reduce stress on the membrane.

Intensity and Number weighting of DLS data do not rely on a monodispersity assumption but treat data as distributions of different-sized particles in solution and allow for more complex assessment of a multi-component system. As such, the most prominent peak was plotted from the distributions and compared using two-way ANOVA. The temperature-dependent trend in HD is similar to the Z-average trend when the data is Number-weighted and Intensity-weighted, except that the data for the 60 °C saturated particles are significantly greater than both the 20 °C and 50 °C data (Figure 5B, 5C). Using these two data-weighting methods there is also no significance observed when comparing the liposomes to the reconstitution samples regardless of temperature which is notably different than what is observed for the Z-average data (Figure 5B,5C).

This is interesting because in Figures 2-3 the increased absorbance was observed only for the 60 °C saturated samples, which implies the involvement of the cloud point of Triton X-100 in the increased extinction observed. As discussed for the liposome saturation studies, surpassing this cloud point during reconstitution protocols might also result in large intermolecular aggregates which could explain the 50 °C and 60 °C-saturated samples' high Z-average HD. If so, Triton X-100 aggregates formed because of the temperature surpassing this cloud point likely make up a small population in the solution that while having limited effect on the number-weighted and intensity-weighted diameters would naturally skew the Z-average distribution towards larger diameter and increase the polydispersity index as is seen in Figure 5 and Supplementary Figure S3.

5.7. FCS ANALYSIS HELPS TO UNDERSTAND LOCALIZATION OF RECONSTITUTED PROTEINS IN COMPLEX PARTICLE – AGGREGATE SOLUTIONS

FCS analysis of the "dye reconstitution" and "protein reconstitution" samples revealed no significant difference in the diffusion coefficients of these fluorescent particles across the three saturation temperatures (Figure 6A). Unlike what was reported by DLS, the diffusion coefficients measured by FCS for the fluorescent particles in the 50°C and 60 °C saturated samples are not significantly different than those for the other temperatures. In fact, the mean HDs of the fluorescent particles in solution obtained from these diffusion coefficients are notably smaller than those measured by DLS, which analyzes both fluorescent and non-fluorescent particles (Supplementary Figure S4A). Additionally, the fluorescent protein reconstitution samples prepared using 20 °C saturation had a median particle number that was greater by at least an order of magnitude than those protein reconstitution samples prepared by saturation at 50°C and 60°C. Together, these data suggest that the large aggregates noticed in DLS data for the 50 °C and 60 °C saturated samples are either not fluorescent and do not incorporate proteins to a significant degree, or they are fluorescent

but have precipitated out of solution as protein-containing aggregates.

The brightness per particle analysis of FCS data reported on how many "protein" brightness equivalents were on average reconstituted into each particle for "dye reconstitution" and "protein reconstitution" samples (Figure 6B). Despite the lack of statistical significance which is an unfortunate result of low signal to noise in the FCS data, the "protein reconstitution" samples have a clearly greater overall particle brightness compared to the "dye reconstitution" samples which confirms that proteins reconstituted into the membranes are responsible for the "protein reconstitution" sample fluorescence. Importantly, the brightness per particle is represented as the raw particle brightness divided by the brightness of freely diffusing spike proteins, so this reports also on the average number of proteins reconstituted in each liposome. No significant difference is shown when comparing the brightness per particle of the "protein reconstitution" samples prepared at the three saturation temperatures, which suggests that the temperature of Triton X-100 saturation does not have a significant impact on the number of proteins reconstituted into each liposome.

6. Conclusions

While reports exist in literature studying how temperature influences Triton X-100 – liposome interactions, studies of how detergent-treatment temperature influences detergent-mediated protein reconstitution are few to none. Here, we present a study exploring the effects of manipulating temperature during Triton X-100 saturation of multicomponent liposomes during proteoliposome production. We demonstrate that saturating these mixed-phase liposomes at room temperature (20°C) versus a temperature above the phase transition temperature for some of the lipids (50°C) does not significantly affect the molar ratio of detergent to lipid required for saturation. At 60°C, however, liposome saturation with Triton X-100 forms micrometer-sized lipid-detergent aggregates that appear largely insoluble under the experimental conditions, which we attribute to cloud-point aggregation of the detergent. Interestingly, the temperature does not seem to influence the effectiveness of BioBead adsorbents in removing similar Triton X-100 concentrations from the solution. Additionally, we present here a simple assay for monitoring BioBead-mediated detergent removal which can spectrophotometrically monitor the number of additions of BioBeads required to remove Triton X-100 from a liposome solution (which in this case was only one). At elevated saturation temperatures (60°C), however, the light scattering component of the extinction measurements dominates the signal and obfuscates this assay, which might suggest that aggregates are coming out of solution and preventing accurate measurement. Reconstitution studies using SARS CoV-2 Spike glycoproteins support the theory that particle aggregation behavior is both temperature- and detergent - dependent, with detergent-free particles at all temperatures failing to aggregate. Finally, FCS analysis provides insight into the localization of reconstituted proteins within complex particle-aggregate solutions and suggests that temperature of Triton X-100 saturation of liposomes does not influence the number of proteins reconstituted per proteoliposome particle. The total number of proteoliposomes formed during this process, however, appears temperature dependent as the 20°C-saturated samples produce proteoliposomes with concentrations over 10x higher than the 50°C and 60°C-saturated samples.

This highlights the key point of this study which is that when designing multi-step protocols involving detergents, lipids, and proteins, it is essential to heed the physical properties of all involved parties. Elements such as the liposome composition, biophysical properties of detergents, buffer compositions and temperature are just some of the interdependent factors that may influence liposome saturation and protein reconstitution. Discussions of such factors cannot definitively explain why the elevated R_{SAT} values are observed in this current

study, and clearly more robust experimentation and formulation-specific analysis would be necessary to fully grasp the mechanisms of these interactions, however this work did provide a set of working conditions within which saturation could be achieved and proteins reconstituted without causing significant aggregation (room temperature saturation, R_T 4.6-9.2). Future work should incorporate more sensitive monitoring techniques that do not depend on light scattering. In addition, by increasing concentrations of all reagents and thereby scaling up the production of particles, more delicate control of BioBead to detergent ratios can be achieved and the saturation and solubilization points can be more clearly distinguished from the critical micelle concentration of the detergent. Despite these limitations, this study serves as a novel guide and example of using multiple analytical methods to optimize preparatory conditions and evaluate the success of detergent mediated protein reconstitution protocols.

Supplementary Materials:

The following supporting information can be downloaded at: https://doi.org/10.5683/SP3/FTIK6H, Figure S1: title; Table S1: title; Video S1: title.

Author Contributions:

SM designed study, executed experiments, analyzed date, drafted manuscript; DC consulted in study and edited manuscript

Funding:

Funding and infrastructure for this study was provided by the National Science and Engineering Research Council of Canada (NSERC Grant #RT691164 to DTC, PGS-D scholarship to SM), Toronto Metropolitan University

Acknowledgements:

We would like to acknowledge the Keenan Research Centre for Biomedical Science Core Facilities at St. Michael's Hospital (Toronto, Canada). Schematics in Figure 1 and graphical abstract were created with BioRender.com.

Institutional Review Board Statement:

Not Applicable

Informed Consent Statement:

Not Applicable

Data Availability Statement:

The original contributions presented in the study are included in the article/supplementary material, further inquiries can be directed to the corresponding author/s.

Conflicts of Interest:

None

References:

1. Lyukmanova, E. N. *et al.* Lipid–protein nanodiscs for cell-free production of integral membrane proteins in a soluble and folded state: Comparison with detergent micelles, bicelles and liposomes. *Biochimica et Biophysica Acta (BBA) - Biomembranes* **1818**, 349–358 (2012).

2. Puthenveetil, R. & Vinogradova, O. Solution NMR: A powerful tool for structural and functional studies of membrane proteins in reconstituted environments. *The Journal of Biological Chemistry* **294**, 15914–15914 (2019).

3. Bibow, S., Hiller, S., Bibow, S. & Hiller, S. A guide to quantifying membrane protein dynamics in lipids and other native-like environments by solution-state NMR spectroscopy. *The FEBS Journal* **286**, 1610–1623 (2019).

4. Meng, S. *et al.* Expression, purification, and reconstitution of small-conductance mechanosensitive channel into lipid bilayer: ready for solid-state NMR study. *Protein Expression and Purification* **240**, 106897 (2026).

5. Du, Z. *et al.* Cryo-EM structure and dynamic basis of phosphate uptake by PHT1 in rice. *Developmental Cell* **61**, 164-177.e6 (2026).

6. Oppedisano, F., Pochini, L., Galluccio, M., Cavarelli, M. & Indiveri, C. Reconstitution into liposomes of the glutamine/amino acid transporter from renal cell plasma membrane: functional characterization, kinetics and activation by nucleotides. *Biochimica et Biophysica Acta (BBA) - Biomembranes* **1667**, 122–131 (2004).

7. Tonazzi, A., Galluccio, M., Oppedisano, F. & Indiveri, C. Functional reconstitution into liposomes and characterization of the carnitine transporter from rat liver microsomes. *Biochimica et Biophysica Acta (BBA) - Biomembranes* **1758**, 124–131 (2006).

8. A~ta, B., Koetters, P. J., Chou, H.-F. & Jonas, A. J. BB. Bioch i f i c~a Reconstitution of lysosomal sulfate transport in proteoliposomes. *Biophysica Acta* **1244**, 311–316 (1995).

9. Zhou, X. L., Chan, C. W. M., Saimi, Y. & Kung, C. Functional reconstitution of ion channels from Paramecium cortex into artificial liposomes. *The Journal of Membrane Biology* **144**, 199–208 (1995).

10. Nomura, T., Cox, C. D., Bavi, N., Sokabe, M. & Martinac, B. Unidirectional incorporation of a bacterial mechanosensitive channel into liposomal membranes. *FASEB J* **29**, 4334–4345 (2015).

11. Wang, X., Berkowitz, G. A. & Peters, J. S. K+-conducting ion channel of the chloroplast inner envelope: functional reconstitution into liposomes. *Proc Natl Acad Sci U S A* **90**, 4981–4985 (1993).

12. Ciancaglini, P. *et al.* Proteoliposomes in nanobiotechnology. *Biophysical Reviews* **4**, 67–67 (2012).

13. Wholey, W. Y. *et al.* Synthetic Liposomal Mimics of Biological Viruses for the Study of Immune Responses to Infection and Vaccination. *Bioconjugate chemistry* **31**, 685–697 (2020).

14. Vaz, R., Freitas, N., Sales, M. G. F. & Frasco, M. F. Photonic hydrogels for monitoring extracellular vesicle mimics. *Biosensors and Bioelectronics* **296**, 118316 (2026).

15. Pereira, S. C. *et al.* Liposome-assisted cystic fibrosis transmembrane conductance regulator delivery to human spermatozoa. *Biomedicine & Pharmacotherapy* **195**, 118981 (2026).

16. Klacsová, M. *et al.* Microalgae-derived vesicles as potential carriers for therapeutic biomacromolecules. *Journal of Drug Delivery Science and Technology* **117**, 107985 (2026).

17. Xu, X. *et al.* Engineering bacterial membrane vesicles: A new paradigm in biomedical innovation. *Coordination Chemistry Reviews* **543**, 216895 (2025).

18. Chen, X. *et al.* Neutrophil-derived proteoliposomes loading doxorubicin and porphyrin for targeted chemo-phototherapy of triple-negative breast cancers. *International Journal of Biological Macromolecules* **339**, 149889 (2026).

19. Smirnova, I. A., Ädelroth, P. & Brzezinski, P. Extraction and liposome reconstitution of membrane proteins with their native lipids without the use of detergents. *Scientific Reports* **8**, 1–7 (2018).

20. Seddon, A. M., Curnow, P. & Booth, P. J. Membrane proteins, lipids and detergents: not just

a soap opera. *Biochimica et Biophysica Acta (BBA) - Biomembranes* **1666**, 105–117 (2004).

21. Ollivon, M., Lesieur, S., Grabielle-Madelmont, C. & Paternostre, M. Vesicle reconstitution from lipid–detergent mixed micelles. *Biochimica et Biophysica Acta (BBA) - Biomembranes* **1508**, 34–50 (2000).

22. Liguo, W. & Lige, T. SCIENCE CHINA Membrane protein reconstitution for functional and structural studies membrane protein, reconstitution, Ca 2+ signaling, Ca 2+ mediators, Ca 2+-regulated enzymes, Ca 2+ transducers Citation: Wang LG, Tonggu LG. Membrane protein reconstitution for functional and structural studies. *REVIEW •. Sci China Life Sci* **58**, 66–74 (2015).

23. Lichtenberg, D., Robson, R. J. & Dennis, E. A. Solubilization of phospholipids by detergents. Structural and kinetic aspects. *Biochim Biophys Acta* **737**, 285–304 (1983).

24. Neves, P. *et al.* Characterization of membrane protein reconstitution in LUVs of different lipid composition by fluorescence anisotropy. *Journal of Pharmaceutical and Biomedical Analysis* **49**, 276–281 (2009).

25. Kloda, A., Lua, L., Hall, R., Adams, D. J. & Martinac, B. Liposome Reconstitution and Modulation of Recombinant N-Methyl-D-Aspartate Receptor Channels by Membrane Stretch. *Source* **104**, 1540–1545 (2007).

26. Mouro-Chanteloup, I. *et al.* Functional Reconstitution into Liposomes of Purified Human RhCG Ammonia Channel. https://doi.org/10.1371/journal.pone.0008921 doi:10.1371/journal.pone.0008921.

27. Girard, P. *et al.* A new method for the reconstitution of membrane proteins into giant unilamellar vesicles. *Biophys J* **87**, 419–429 (2004).

28. Lévy, D., Gulik, A., Bluzat, A. & Rigaud, J. L. Reconstitution of the sarcoplasmic reticulum Ca2+-ATPase: mechanisms of membrane protein insertion into liposomes during reconstitution procedures involving the use of detergents. *BBA - Biomembranes* **1107**, 283–298 (1992).

29. Jayachandran, D., Banerjee, S. & Chundawat, S. P. S. Plant cellulose synthase membrane protein isolation directly from Pichia pastoris protoplasts, liposome reconstitution, and its enzymatic characterization. *Protein Expression and Purification* **210**, 106309–106309 (2023).

30. Kruip, J., Karapetyan, N. V., Terekhova, I. V. & Rögner, M. In vitro oligomerization of a membrane protein complex. Liposome-based reconstitution of trimeric photosystem I from isolated monomers. *Journal of Biological Chemistry* **274**, 18181–18188 (1999).

31. Murray, D. T., Griffin, J. & Cross, T. A. Detergent optimized membrane protein reconstitution in liposomes for solid state NMR. *Biochemistry* **53**, 2454–2463 (2014).

32. Knol, J., Sjollema, K. & Poolman, B. Detergent-mediated reconstitution of membrane proteins. *Biochemistry* **37**, 16410–16415 (1998).

33. Simeonov, P., Werner, S., Haupt, C., Tanabe, M. & Bacia, K. Membrane protein reconstitution into liposomes guided by dual-color fluorescence cross-correlation spectroscopy. *Biophysical Chemistry* **184**, 37–43 (2013).

34. Schwamborn, M., Schumacher, J., Sibold, J., Teiwes, N. K. & Steinem, C. Monitoring ATPase induced pH changes in single proteoliposomes with the lipid-coupled fluorophore Oregon Green 488. *Analyst* **142**, 2670–2677 (2017).

35. Top, D. *et al.* Liposome reconstitution of a minimal protein-mediated membrane fusion machine. *EMBO Journal* **24**, 2980–2988 (2005).

36. McColman, S. *et al.* SARS-CoV-2 virus-like-particles via liposomal reconstitution of spike glycoproteins. *Nanoscale advances* **5**, 4167–4181 (2023).

37. Himbert, S. *et al.* Erythro-VLPs: Anchoring SARS-CoV-2 spike proteins in erythrocyte liposomes. *PLoS ONE* **17**, e0263671–e0263671 (2022).

38. Stubičar, N., Matejaš, J., Zipper, P. & Wilfing, R. Size, Shape and Internal Structure of Triton X-100 Micelles Determined by Light and Small-Angle X-Ray Scattering Techniques. *Surfactants in Solution* 181–195 (1989) doi:10.1007/978-1-4615-7984-7_10.

39. Wexler, A. S. Determination of Phenolic Substances by Ultraviolet Difference Spectroscopy. *Analytical Chemistry* **35**, 1936–1943 (1963).

40. Tiller, G. E., Mueller, T. J., Dockter, M. E. & Struve, W. G. Hydrogenation of triton X-100 eliminates its fluorescence and ultraviolet light absorption while preserving its detergent properties. *Analytical biochemistry* **141**, 262–266 (1984).

41. Akhlaghi, N. & Riahi, S. Salinity Effect on the Surfactant Critical Micelle Concentration through Surface Tension Measurement. *Iranian Journal of Oil and Gas Science and Technology* **8**, 50–63 (2019).

42. M'Baye, G., Mély, Y., Duportail, G. & Klymchenko, A. S. Liquid Ordered and Gel Phases of Lipid Bilayers: Fluorescent Probes Reveal Close Fluidity but Different Hydration. *Biophysical Journal* **95**, 1217–1217 (2008).

43. Redondo-Morata, L., Giannotti, M. I. & Sanz, F. Influence of cholesterol on the phase transition of lipid bilayers: A temperature-controlled force spectroscopy study. *Langmuir* **28**, 12851–12860 (2012).

44. Márquez, M. G. & Sterin-Speziale, N. B. Is DRM lipid composition relevant in cell-extracellular matrix adhesion structures? *Cell Adhesion & Migration* **2**, 180–180 (2008).

45. Arnulphi, C. *et al.* Triton X-100 partitioning into sphingomyelin bilayers at subsolubilizing detergent concentrations: Effect of lipid phase and a comparison with dipalmitoylphosphatidylcholine. *Biophysical Journal* **93**, 3504–3514 (2007).

46. Patra, S. K., Alonso, A. & Goñi, F. M. Detergent solubilisation of phospholipid bilayers in the gel state: the role of polar and hydrophobic forces. *Biochimica et Biophysica Acta (BBA) - Biomembranes* **1373**, 112–118 (1998).

47. López, O. *et al.* Direct formation of mixed micelles in the solubilization of phospholipid liposomes by Triton X-100. *FEBS Letters* **426**, 314–318 (1998).

48. Lichtenberg, D., Ahyayauch, H., Alonso, A., Lix, F. & Goñ, M. Detergent solubilization of lipid bilayers: a balance of driving forces. *Trends in Biochemical Sciences* **38**, 85–93 (2013).

49. Urbaneja, M. A., Nieva, J. L., Goñi, F. M. & Alonso, A. The influence of membrane composition on the solubilizing effects of Triton X-100. *Biochimica et Biophysica Acta (BBA) - Biomembranes* **904**, 337–345 (1987).

50. Grzybek, M., Kubiak, J., Łach, A., Przybyło, M. & Sikorski, A. F. A Raft-Associated Species of Phosphatidylethanolamine Interacts with Cholesterol Comparably to Sphingomyelin. A Langmuir-Blodgett Monolayer Study. https://doi.org/10.1371/journal.pone.0005053 doi:10.1371/journal.pone.0005053.

51. Morel, E. *et al.* Cholesterol trafficking and raft-like membrane domain composition mediate scavenger receptor class B type 1-dependent lipid sensing in intestinal epithelial cells. *Biochimica et Biophysica Acta (BBA) - Molecular and Cell Biology of Lipids* **1863**, 199–211 (2018).

52. Manni, M. M., Cano, A., Alonso, C. & Goñi, F. M. Lipids that determine detergent resistance of MDCK cell membrane fractions. *Chemistry and Physics of Lipids* **191**, 68–74 (2015).

53. Björkbom, A. *et al.* Characterization of membrane properties of inositol phosphorylceramide. *Biochimica et Biophysica Acta (BBA) - Biomembranes* **1798**, 453–460 (2010).

54. Arkhipov, V. P., Arkhipov, R. V., Kuzina, N., Petrova, E. V. & Filippov, A. Aggregation Properties of Triton X-100 in a Mixture of Ordinary and Heavy Water. *Applied Magnetic Resonance* **54**, 415–425 (2023).

55. Alam, M. S., Siddiq, A. M. & Mandal, A. B. The Micellization and Clouding Phenomena of a Nonionic Surfactant, Poly(ethylene glycol) t-octylphenyl ether (Triton X-100): Effect of (Chloride Salt) Electrolytes. *Journal of Dispersion Science and Technology* **37**, 1287–1293 (2016).

56. Lévy, D., Bluzat, A., Seigneuret, M. & Rigaud, J. L. A systematic study of liposome and proteoliposome reconstitution involving Bio-Bead-mediated Triton X-100 removal. *Biochimica et Biophysica Acta (BBA) - Biomembranes* **1025**, 179–190 (1990).

57. Rigaud, J. L. *et al.* Bio-Beads: An Efficient Strategy for Two-Dimensional Crystallization of Membrane Proteins. *Journal of Structural Biology* **118**, 226–235 (1997).

58. Rigaud, J.-L., Levy, D., Mosser, G. & Lambert, O. Detergent removal by non-polar polystyrene beads. *European Biophysics Journal* **27**, 305–319 (1998).

59. Kollmitzer, B., Heftberger, P., Rappolt, M. & Pabst, G. Monolayer spontaneous curvature of raft-forming membrane lipids. *Soft Matter* **9**, 10877–10884 (2013).